Inorganic Chemistry

Article

Relevance of the Ligand Exchange Rate and Mechanism of *fac*-[(CO)₃M(H₂O)₃]⁺ (M = Mn, Tc, Re) Complexes for New Radiopharmaceuticals

Pascal V. Grundler,[†] Lothar Helm,*,[†] Roger Alberto,*,[‡] and André E. Merbach[†]

Institut des Sciences et Ingénierie Chimiques, Ecole Polytechnique Fédérale de Lausanne, BCH, CH-1015 Lausanne, Switzerland, and Anorganisch-chemisches Institut, Universität Zürich, Winterthurerstrasse 190, CH-8057 Zürich, Switzerland

The water exchange process on *fac*-[(CO)₃Mn(H₂O)₃]⁺ and *fac*-[(CO)₃Tc(H₂O)₃]⁺ was kinetically investigated by ¹⁷O NMR as a function of the acidity, temperature, and pressure. Up to pH 6.3 and 4.4, respectively, the exchange rate is not affected by the acidity, thus demonstrating that the contribution of the monohydroxo species *fac*-[(CO)₃M-(OH)(H₂O)₂] is not significant, which correlates well with a higher pK_a for these complexes compared to the homologue *fac*-[(CO)₃Re(H₂O)₃]⁺ complex. The water exchange rate k_{ex}^{298}/s⁻¹ ($\Delta H_{ex}^{\ddagger}$/kJ mol⁻¹; $\Delta S_{ex}^{\ddagger}$/J mol⁻¹ K⁻¹; $\Delta V^{\ddagger}$/cm³ mol⁻¹) decreases down group 7 from Mn to Tc and Re: 23 (72.5; +24.4; +7.1) > 0.49 (78.3; +11.7; +3.8) > 5.4 × 10⁻³ (90.3; +14.5; −). For the Mn complex only, an O exchange on the carbonyl ligand could be measured (k_{CO}^{338} = 4.3 × 10⁻⁶ s⁻¹), which is several orders of magnitude slower than the water exchange. In the case of the Tc complex, the coupling between ¹⁷O ($I = ^5/_2$) and ⁹⁹Tc ($I = ^9/_2$) nuclear spins has been observed ($^1J_{⁹⁹Tc,¹⁷O} = 80 \pm 5$ Hz). The substitution of water in *fac*-[(CO)₃M(H₂O)₃]⁺ by dimethyl sulfide (DMS) is slightly faster than that by CH₃CN: 3 times faster for Mn, 1.5 times faster for Tc, and 1.2 times faster for Re. The pressure dependence behavior is different for Mn and Re. For Mn, the change in volume to reach the transition state is always clearly positive (water exchange, CH₃CN, DMS), indicating an I$_d$ mechanism. In the case of Re, an I$_d$/I$_a$ changeover is assigned on the basis of reaction profiles with a strong volume maximum for pyrazine and a minimum for DMS as the entering ligand.

Introduction

Aquacarbonyl complexes combine two important and, at first glance, perhaps conflicting features. On the one side, they bear carbon monoxide, one of the most important and versatile ligands in the organometallic chemistry of transition metals and, on the other side, they convey water, a ubiquitous molecule in biological and environmental systems that is also praised as a green solvent. Over the last years, aqueous organometallic chemistry has expanded,[1] and thus mechanistic aspects of the reactivity of this category of organo-

metallic complexes deserve particular consideration. Among them, the aquacarbonyl complexes of group 7 elements (Mn, Tc, Re) have gained much attention because of the high stability of the *fac*-{(CO)₃M⁺} fragment.[2] Its stability allowed the extension of the pool of potential Tc-based radiopharmaceuticals to complexes with low-valent Tc. Furthermore, Re has been investigated not only as a model for Tc but also as a potential radiotherapeutic agent with its β⁻-emitting isotope ¹⁸⁸Re, which is complementary to the diagnostic use of ⁹⁹ᵐTc.[3] Although the triaquacarbonyl complexes are not directly practical radiopharmaceuticals, they are the precursors in the aqueous preparation of bioconjugate complexes. From this point of view, their kinetic behavior is an especially important aspect that determines the preparation, uptake, and clearance of the radiopharmaceutical agents. The kinetic

* To whom correspondence should be addressed. E-mail: lothar.helm@epfl.ch (L.H.), ariel@aci.unizh.ch (R.A.).
† Ecole Polytechnique Fédérale de Lausanne.
‡ Universität Zürich.

(1) (a) Koelle, U. *Coord. Chem. Rev.* **1994**, *13516*, 623. (b) *Aqueous-Phase Organometallic Catalysis*; Cornils, B., Hermann, W. A., Eds.; Wiley-VCH: Weinheim, Germany, 1998. (c) Helm, L.; Merbach, A. E. *Chem. Rev.* **2005**, *105*, 1923. (d) Richens, D. T. *Chem. Rev.* **2005**, *105*, 1961.

(2) Alberto, R.; Schibli, R.; Waibel, R.; Abram, U.; Schubiger, A. P. *Coord. Chem. Rev.* **1999**, *192*, 901.
(3) Alberto, R. *Eur. J. Nucl. Med. Mol. Imaging* **2003**, *30*, 1299.

behavior of [(CO)₃Re(H₂O)₃]⁺ has been recently described,[4] showing that the ligand substitution mechanism is depending on the nature of the entering ligand,[5] and for [(CO)₃Tc(H₂O)₃]⁺, kinetic data for the substitution of water molecules by carbon monoxide have already been reported.[6] An investigation of the homologous manganese(I) triaqua-carbonyl complex has highlighted some interesting kinetic features of this complex,[7] which motivated us to include it in the present investigation. Hence, a comparison over the whole group 7 is possible, which is one of the few cases where the complete set of homologous complexes is available for study. Besides radiopharmaceutical aspects, a new field in low-valent Tc complexes is gaining interest because it has been shown that they can also play a role in the remediation efforts of waste material from Pu production.[8]

In the present work, the kinetics of water exchange and substitution on [(CO)₃M(H₂O)₃]⁺ (M = Mn, Tc, Re) complexes have been systematically investigated by multi-nuclear NMR. The results reveal the reactivity trend within the group and also permit comparisons with analogous complexes for elements of groups 6 and 8, i.e., Cr(0), W(0), and Ru(II).

Experimental Section

Chemicals and Syntheses. Silver trifluoromethanesulfonate (98%), acetonitrile (99.5% p.a.), dimethyl sulfide (DMS), 2-mor-pholinoethanesulfonic acid monohydrate (MES; 99.5%), and piperazine-1,4-bis(2-ethanesulfonic acid) (PIPES; 99%) were purchased from Fluka. Trifluoromethanesulfonic acid (99%), bromopenta-carbonylmanganese(I) (98%), and manganese(II) perchlorate hexahydrate (99%) were obtained from Acros. Perchloric acid (70−72% p.a.) and sodium perchlorate monohydrate (99% p.a.) were purchased from Merck. Piperazine-*N,N'*-bis(4-butanesulfonic acid) (PIPBS; 95%) was obtained from GFS Chemicals (Columbus, OH). Sodium (trimethylsilyl)propanesulfonate (TMSPS) was purchased from Ciba-Geigy. ¹⁷O-enriched water, H₂¹⁷O, was obtained from the National High Technology Centre of Georgia (20.9% ¹⁷O, 3.9% ¹⁸O; 10.5% ¹⁷O, 49.3% ¹⁸O). Solutions made of commercially available sodium trifluoromethanesulfonate were found to be basic, due to alkaline traces. Therefore, this salt was prepared by neutralizing trifluoromethanesulfonic acid with sodium hydroxide (NaOH).

A new and simple way to prepare an aqueous solution of [(CO)₃Mn(H₂O)₃]⁺ has been used. A first step is the preparation of (CF₃SO₃)Mn(CO)₅ from BrMn(CO)₅.[9] In a second step, this complex is dissolved in degassed water of the desired acidity to produce by hydrolysis solutions of the aqua ion. The compositions of those solutions were confirmed by IR (2050 and 1945 cm⁻¹) and ¹⁷O NMR (−65 ppm) spectroscopy. The advantage over the

method proposed by Prinz et al.,[7] which consists of refluxing (CF₃SO₃)Mn(CO)₅ in acetone to produce [(CO)₃Mn(acetone)₃]-(CF₃SO₃) and subsequent hydrolysis, is to avoid impurities resulting from the use of acetone (diacetone alcohol) and Mn(II), which require tedious ion-exchange separation and produce always very acidic solutions (CF₃SO₃H as an eluent). Another route involving first the preparation of [(CO)₃MnX₃](NR₄)₂ from XMn(CO)₅ (X = Cl, Br; R = Me, Et), followed by hydrolysis, was attempted. Successful for the Re analogue,[10] it failed for Mn. Because the Mn(I) complexes are light-sensitive, all steps were performed in a dark room with minimal red lighting (Philips PF712E 15-W bulb) and under N₂. Prior to kinetic measurements, [(CO)₃Mn(H₂O)₃]⁺ concentrations of the stock solutions were determined by UV−vis spectroscopy (λ_{max} = 387 nm; ϵ_{387} = 1600 M⁻¹ cm⁻¹).[11]

The complex [NEt₄]₂[⁹⁹TcCl₃(CO)₃] was prepared as described elsewhere.[12] The complex was dissolved in 0.1 M HClO₄, and the halides precipitated by the addition of an 0.1 M HClO₄ solution of AgClO₄. AgCl was filtered off and the solution containing [⁹⁹Tc(OH₂)₃(CO)₃]⁺ used for the experiments without further treatment. The ⁹⁹Tc concentration of the stock solution was determined by scintillation counting. [⁹⁹Tc(OH₂)₃(CO)₃]⁺ solutions of various acidity were obtained by partially neutralizing HClO₄ of the stock solution with NaOH and adding an adequate buffer when required. [H⁺] was checked with a glass electrode. ***Caution!*** *⁹⁹Tc emits low-energy β particles with a half-life of 2.13 × 10⁵ years. Because the low-energy β particles do not penetrate glass walls, no special shielding is required; however, special care is required when manipulating radioactive materials to avoid contamination and incorporation. Perchlorates are potentially explosive in the presence of organic compounds, especially when H⁺ is present, and under anhydrous conditions and heat.*

Solutions of [(CO)₃Re(H₂O)₃]CF₃SO₃ were prepared as described earlier.[5]

Stock Solutions of the Ligands. With DMS being very volatile, it was not possible to take a well-known amount of this compound to prepare an aqueous solution. A saturated solution of DMS was prepared, and aliquots of this solution were diluted to obtain solutions of the appropriate concentration. Finally, the concentration was checked from ¹H NMR integration using TMSPS as an internal quantitative reference when a precise knowledge of the concentration was required.

NMR Measurements. NMR spectra were recorded on Bruker ARX-400 and DPX-400 spectrometers. The ¹⁷O, ⁹⁹Tc, and ¹H and ¹³C NMR chemical shifts are referenced to bulk water, TcO₄⁻, and tetramethylsilane, respectively, and measured with respect to nitromethane (605 ppm), [(CO)₃Tc(H₂O)₃]⁺ (−868 ppm), and tetraethylammonium (¹H methyl 1.25 ppm, ¹³C methylene 54.4 ppm), respectively. The signal of bulk water was suppressed either by adding a paramagnetic Mn(II) salt to the solutions or by applying the 1, −3, 3, 1[13] or inversion−recovery[14] pulse sequences.

For exchange and substitution kinetics on [(CO)₃Tc(H₂O)₃]⁺, a home-built fast-injection device was used.[15] This apparatus allows

(4) Grundler, P. V.; Salignac, B.; Cayemittes, S.; Alberto, R.; Merbach, A. E. *Inorg. Chem.* **2004**, *43*, 865.
(5) Salignac, B.; Grundler, P. V.; Cayemittes, S.; Frey, U.; Scopelliti, R.; Merbach, A. E.; Hedinger, R.; Hegetschweiler, K.; Alberto, R.; Prinz, U.; Raabe, G.; Kölle, U.; Hall, S. *Inorg. Chem.* **2003**, *42*, 3516.
(6) Aebischer, N.; Schibli, R.; Alberto, R.; Merbach, A. E. *Angew. Chem., Int. Ed.* **2000**, *39*, 254.
(7) Prinz, U.; Koelle, U.; Ulrich, S.; Merbach, A. E.; Maas, O.; Hegetschweiler, K. *Inorg. Chem.* **2004**, *43*, 2387.
(8) Lukens, W. W.; Shuh, D. K.; Schroeder, N. C.; Ashley, K. R. *Environ. Sci. Technol.* **2004**, *38*, 229.
(9) Schmidt, S. P.; Nitschke, J.; Trogler, W. C. *Inorg. Synth.* **1989**, *26*, 113.
(10) Alberto, R.; Egli, A.; Abram, U.; Hegetschweiler, K.; Gramlich, V.; Schubiger, P. A. *J. Chem. Soc., Dalton Trans.* **1994**, 2815.
(11) Prinz, U. Ph.D. Thesis, RWTH Aachen, Aachen, Germany, Aachener Beiträge zur Chemie, Band 19, Wissenschaftsverlag Mainz in Aachen, 2000.
(12) Alberto, R.; Schibli, R.; Egli, A.; Abram, U.; Kaden, T. A.; Schubiger, P. A. *J. Am. Chem. Soc.* **1998**, *120*, 7987.
(13) (a) Hore, P. J. *J. Magn. Reson.* **1983**, *54*, 539. (b) Hore, P. J. *J. Magn. Reson.* **1983**, *55*, 283.
(14) Günther, H. *NMR Spectroscopy*, 2nd ed.; John Wiley & Sons: Chichester, U.K., 1992.
(15) Bernhard, P.; Helm, L.; Ludi, A.; Merbach, A. E. *J. Am. Chem. Soc.* **1985**, *107*, 312.

mixing inside the NMR spectrometer, in less than 1 s, of ^{17}O-enriched water or a solution of the ligand from a thermostated syringe with a solution of complex already in the NMR tube and then following at once the reaction by NMR.

^{17}O (^{99}Tc) acquisition parameters for the fast-injection experiment with $[(CO)_3Tc(H_2O)_3]^+$ were as follows: 35 (16) μs pulse length, 64 scans accumulated over a spectral width of 22 (50) kHz with 800 (8K) data points. A repetition rate of 22 (100) ms allowed the recording of a spectrum every 1.4 (6.4) s.

For all kinetics, the temperature in the NMR probe was measured by a substitution technique using a 100-Ω Pt resistor.[16] For variable-pressure measurements, a home-built high-pressure NMR probe was used.[17]

IR and UV−Vis Measurements. IR spectra were recorded on a Spectrum One Fourier transform IR spectrometer from Perkin-Elmer equipped with a Diamond ATR Golden Gate sampling accessory. Spectrophotometric UV−vis data were collected on a Perkin-Elmer Lambda-19 double-beam spectrometer using 10-mm cells.

Kinetic Data Treatement. Kinetic experiments were conducted in the cases of Tc (high temperature) and Mn by monitoring the NMR signals' line shapes as a function of temperature. For ligand substitution on Mn, the line widths were corrected for inhomogeneity by subtracting the line width of the (trimethylsilyl)propanesulfonate signal used as the reference (^{1}H NMR). For ^{17}O NMR, the signal of the carbonyl O atom was used as a reference (natural width ∼20 Hz at 340 K). ^{17}O enrichment of the carbonyl ligand was achieved by heating the ^{17}O-enriched aqueous sample overnight to 340 K prior to line-width measurements.

The evolution of the NMR signals' intensities as a function of time was monitored in the cases of Tc (low temperature) and Re. Integrals of these signals were obtained by fitting a Lorentzian function to the signals with the program *NMRICMA 3.0* running under *MATLAB*.[18] Parameters of the adequate equations were least-squares-fitted to these experimental data using the program suite *VISUALISEUR−OPTIMISEUR* running under *MATLAB*.[19]

Results

Water Exchange Kinetics on $[(CO)_3Mn(H_2O)_3]^+$. The water exchange process on the Mn complex (eq 1) is fast enough to produce a line broadening of the signal of bound water in ^{17}O NMR. The signals of bound (-65 ppm) and free water are still well resolved; therefore, the NMR slow-exchange condition is satisfied.

$$[(CO)_3Mn(H_2O)_3]^+ + 3H_2{}^*O \rightleftharpoons [(CO)_3Mn(H_2{}^*O)_3]^+ + 3H_2O \quad (1)$$
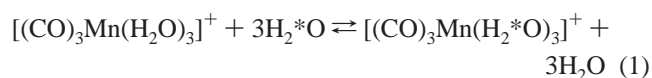
Suppression of the much more intense bulk water signal was achieved with 1, -3, 3, 1 or inversion−recovery pulse sequences,[13,14] which increased significantly the quality of the spectra and allowed one to determine with good accuracy the line width of the bound water signal.

In the domain of slow exchange, the observed transverse relaxation rate ($1/T_{2obs}$), which is proportional to the line width ($\pi W_{obs} = 1/T_{2obs}$), is the sum of two contributions: the water exchange process and the ^{17}O quadrupolar relaxation ($1/T_{2Q}$) as written in eq 2.

$$\frac{1}{T_{2obs}} = \frac{1}{\tau_{obs}} + \frac{1}{T_{2Q}} \quad (2)$$

τ_{obs} is the mean residence time of a water molecule in the first coordination sphere of the triaqua ion, and its inverse, $1/\tau_{obs}$, is equal to the first-order rate constant for the exchange, k_{obs}, of a particular water molecule. If the complex undergoes hydrolysis, the water exchange will also take place on the hydrolyzed species. The observed k_{obs} is then the sum of two contributions as shown in eq 3, where k_{ex} is the water exchange rate on the triaqua ion and k_2 that on the hydrolyzed complex.

$$k_{obs} = k_{ex} + k_2/[H^+] \quad (3)$$

The temperature dependences of the water exchange rates and $1/T_{2Q}$ are described by the Eyring equation (eq S1 in the Supporting Information) and the Arrhenius law (eq S2 in the Supporting Information), respectively. Monitoring the line width, as a function of temperature, allows one to determine the activation parameters. Consequently, solutions of the complex covering an acidity range from $[H^+] = 0.4$ M to $[H^+] = 5 \times 10^{-7}$ M were studied (Tables S1−S5 in the Supporting Information).

However, the poor stability of the complex at elevated temperature (>50 °C) and lower acidities were drawbacks to the successful completion of these experiments. The decomposition of $[(CO)_3Mn(H_2O)_3]^+$, yielding the paramagnetic Mn^{2+} aqua ion, could easily be detected by NMR because of the broadening of the bulk water peak. Nevertheless, the line width of the bound water remained unaffected by the presence of the paramagnetic Mn^{2+} aqua ion. Checking the acidity of the NMR samples with a combined glass electrode revealed that the acidity was decreasing as the complex decomposed. Most probably, Mn(I) reduces the protons of water to H_2 (eq 4).

$$[(CO)_3Mn(H_2O)_3]^+ + H^+ \rightarrow Mn(aq)^{2+} + \frac{1}{2}H_2 + 3CO \quad (4)$$
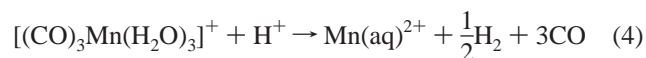
For solutions with $[H^+] < 10^{-4}$ M, the noncomplexing buffers[20] MES and PIPES were used to control the acidity. However, they were not very efficient because of their relatively low solubility compared to the concentration of $[(CO)_3Mn(H_2O)_3]^+$ required for the NMR measurements. As a consequence, the acidity of the samples changed during the measurements. However, systematic checks between each measurement allowed one to track these variations and to stop the measurements when the drop in acidity was no longer negligible.

Individual analysis of the data for each acidity domain showed that k_{obs}^{343}, $\Delta H^\ddagger$, and E_Q are not affected by the

(16) Amman, C.; Meier, P. F.; Merbach, A. E. *J. Magn. Reson.* **1982**, *46*, 319.

(17) Cusanelli, T.; Nicula-Dadci, L.; Frey, U.; Merbach, A. E. *Inorg. Chem.* **1997**, *36*, 221.

(18) Helm, L.; Borel, A. Institut des Sciences et Ingénierie Chimiques, Ecole Polytechnique Fédérale de Lausanne, Switzerland.

(19) Yerly, F. Institut des Sciences et Ingénierie Chimiques, Ecole Polytechnique Fédérale de Lausanne, Switzerland.

(20) Kandegedara, A.; Rorabacher, D. B. *Anal. Chem.* **1999**, *71*, 3140.
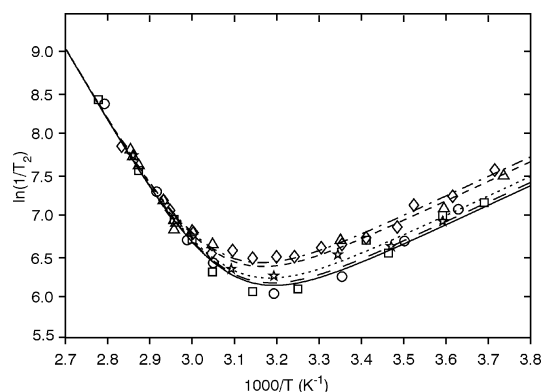
Figure 1. Transverse relaxation rate ($1/T_{2obs}$) temperature dependence of the ¹⁷O NMR signal of bound water in $[(CO)_3Mn(H_2O)_3]^+$ in five different acidity domains: $\bigcirc-$, $[H^+] = 0.4$ M; $\square--$, $[H^+] = (1.2-1.4) \times 10^{-2}$ M; $\diamondsuit-\cdot-$, $[H^+] = (2-3) \times 10^{-4}$ M; $\triangle---$, $[H^+] = (3-6) \times 10^{-5}$ M; $\star\cdots$, $[H^+] = (0.5-1) \times 10^{-6}$ M. Lines represent best fits according to eq 2 and eqs S1 and S2 in the Supporting Information.

acidity change (Table S6 in the Supporting Information). Therefore, in a final fit, all data were analyzed together. For this final fit, common k_{ex}^{343}, $\Delta H^{\ddagger}$, and E_Q and five individual $1/T_{2Q}^{298}$ values were used. The small difference in $1/T_{2Q}$ observed in the low-temperature domain may be related to variation in the viscosity due to small changes in the composition of the solutions (no trend correlated to the acidity is observed). The results are summarized in Table S7 in the Supporting Information, and Figure 1 gives a graphical view of the final fit, which yields the following values: $k_{ex}^{343} = (1.22 \pm 0.04) \times 10^3$ s⁻¹, $\Delta H_{ex}^{\ddagger} = 72.5 \pm 3$ kJ mol⁻¹, $\Delta S_{ex}^{\ddagger} = +24.4 \pm 8$ J mol⁻¹ K⁻¹, and $E_Q = 20.5 \pm 1$ kJ mol⁻¹. Although the acidity is varied over 5 orders of magnitude (p[H⁺] = 1−6), no significant change in the water exchange rate constant is observed.

The activation volume for the water exchange in $[(CO)_3Mn(H_2O)_3]^+$ was determined by variable-pressure ¹⁷O NMR at $[H^+] = 0.1$ M and 339.8 K. $(1/T_{2Q})_P$ values were calculated from $\Delta V_Q^{\ddagger} = +0.3$ cm³ mol⁻¹ (ref 7) and $(1/T_{2Q}^T)_0$ using eq 5 (Table S8 in the Supporting Information).

$$\left(\frac{1}{T_{2Q}}\right)_P = \left(\frac{1}{T_{2Q}}\right)_0 \exp\left(-\frac{P\Delta V_Q^{\ddagger}}{RT}\right) \qquad (5)$$

These values were used to calculate k_{ex} at each pressure. A plot of ln k_{ex} vs P (eq 6) is shown in Figure 2. The linear regression yielded $\Delta V_{ex}^{\ddagger} = +7.1 \pm 2.0$ cm³ mol⁻¹.[21]

$$(k)_P = (k)_0 \exp\left(-\frac{P\Delta V^{\ddagger}}{RT}\right) \qquad (6)$$

Oxygen Exchange on the Carbonyl Ligand of $[(CO)_3Mn(H_2O)_3]^+$. Besides the water exchange, another process is taking place, which is easily observed by ¹⁷O NMR in ¹⁷O-enriched solutions. The O atom of the carbonyl ligands is also exchanging with the solvent. This exchange, already observed,[7] is assumed to proceed via the formation of a metallacarboxylic acid.

This reaction is several orders of magnitude slower than the water exchange and is best observed by monitoring the increase of the carbonyl ¹⁷O signal at 389 ppm. The reaction
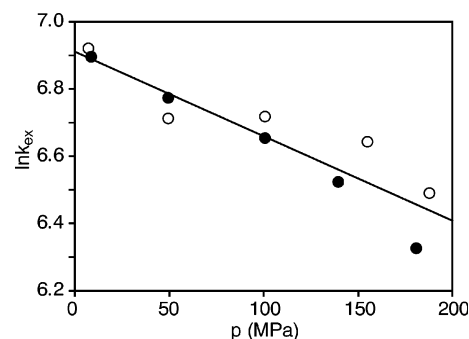
Figure 2. Pressure dependence of the water exchange rate (k_{ex}) on $[(CO)_3Mn(H_2O)_3]^+$ at 339.8 K and $[H^+] = 0.1$ M (two different samples ● and ○).

was followed at 338 K for 19 h (Figure S1 in the Supporting Information). During this time, the carbonyl ¹⁷O signal integral increased to about 25% of the integral of bound water. The rate constant for this exchange could be determined using eq 7, where $I(t)$ is the time-dependent integral of the signal, k_{CO} the first-order exchange rate constant, χ_{∞} the mole fraction of bound O (less than 1%), and I_{∞} the integral at equilibrium.

$$I(t) = I_{\infty}\left[1 - \exp\left(\frac{k_{CO}t}{1 - \chi_{\infty}}\right)\right] \qquad (7)$$

When the parameter k_{CO} of eq 7 was fitted to the experimental data, an exchange rate constant of $(4.3 \pm 0.2) \times 10^{-6}$ s⁻¹ at 338 K was found, which corresponds to a half-life of 1.9 days.

Water Substitution Kinetics on $[(CO)_3Mn(H_2O)_3]^+$. The water molecules of $[(CO)_3Mn(H_2O)_3]^+$ are easily substituted by other ligands. In the presence of acetonitrile, the formation of three new species could be observed by ¹H NMR spectroscopy at +2.389, +2.379, and +2.346 ppm assigned respectively to the mono-, di-, and triacetonitrile complexes (free acetonitrile +2.060 ppm). Similar results were obtained for DMS with peaks at +2.436, +2.492, and +2.520 ppm corresponding respectively to the mono-, bis-, and tris-(dimethyl sulfide) complexes (free DMS +2.110 ppm). Increasing the temperature led to a broadening of the lines of free and bound ligands. For variable-temperature kinetic measurements, ligand concentrations were chosen so as to have only the mono complex and free ligand signals. A ligand/metal ratio of 1:50−60 for acetonitrile and DMS was found to be optimal. TMSPS was used as the internal reference for the line width as well as for the concentration in the case of DMS, with the later being very volatile (bp 36−37 °C).

The substitution reaction shown in eqs 8 and 9 defines the corresponding equilibrium and rate constants (M stands for $[(CO)_3Mn(H_2O)_3]^+$ and ML for $[(CO)_3MnL(H_2O)_2]^+$).

---

(21) In a previous paper,[7] a value of −4.5 cm³ mol⁻¹ was reported from four data points obtained on very dilute solutions requiring the accumulation of a vast number of transients. Thanks to the new synthetic route, the concentration was higher in the new experiments, leading to excellent variable-pressure data.

$$M + L \rightleftharpoons ML + H_2O \qquad (8)$$
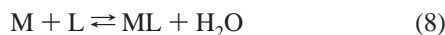
$$K_{f,1} = \frac{[ML]}{[M][L]} = \frac{k_{f,1}}{k_{r,1}} \qquad (9)$$

The relative populations of free and bound ligands are given by $p_L = [L]/([L] + [M])$ and $p_{ML} = [ML]/([L] + [M])$. In the slow-exchange NMR approximation, the residence times of L in the free τ_L and in the bound τ_{ML} states are obtained from the signal line width (eq 2 without the quadrupolar term). The residence times are related to the populations of the two sites by eq 10.

$$p_L/\tau_L = p_{ML}/\tau_{ML} \qquad (10)$$

Assuming a second-order rate law for the complex formation rate, $1/\tau_L$ is proportional to the rate constant $k_{f,1}$ (eq 11) and $1/\tau_{ML}$ is equal to the complex dissociation rate constant $k_{r,1}$ (eq 12).

$$1/\tau_L = k_{f,1}[M] \qquad (11)$$

$$1/\tau_{ML} = k_{r,1} \qquad (12)$$

Significant line broadening occurs only above 310 K and could be followed up to 350 K with CH_3CN and 340 K with DMS. At higher temperatures, the NMR slow exchange approximation is no more valid. The concentration of $[(CO)_3Mn(H_2O)_3]^+$ at each temperature was determined by the difference between the initial concentration of $[(CO)_3Mn(H_2O)_3]^+$ and the concentration of $[(CO)_3MnL(H_2O)_2]^+$ determined from its integral. The equilibrium concentration of $[(CO)_3Mn(H_2O)_3]^+$ is close to the initial concentration because of the small ligand/metal ratio. Thus, it was possible to determine $k_{f,1}$, according to eq 11 (Figure S2 and Tables S9 and S10 in the Supporting Information). The substitution with DMS was found to be twice as fast as that with CH_3CN at 333 K with respectively $k_{f,1}^{333} = 122 \pm 20$ mol^{-1} s^{-1}, $\Delta H_{f,1}^{\ddagger} = 71.2 \pm 12$ kJ mol^{-1}, $\Delta S_{f,1}^{\ddagger} = +8.1 \pm 38$ J mol^{-1} K^{-1} and $k_{f,1}^{333} = 68.9 \pm 5$ mol^{-1} s^{-1}, $\Delta H_{f,1}^{\ddagger} = 83.9 \pm 5$ kJ mol^{-1}, $\Delta S_{f,1}^{\ddagger} = +41.3 \pm 16$ J mol^{-1} K^{-1}.

The equilibrium constants K_1 were determined from 270 to 340 K (Figure S2 and Tables S9 and S10 in the Supporting Information). The concentrations of free and bound ligands were obtained from the integrals of the corresponding signals and the concentration $[(CO)_3Mn(H_2O)_3]^+$ as above. When $k_{r,1}$ was available, the equilibrium constants were also calculated from $k_{f,1}$ and $k_{r,1}$ and found to correspond within experimental error to the values obtained from the integrals, and thus the average values have been used to calculate the reaction enthalpies ($\Delta H_{f,1}$) and entropies ($\Delta S_{f,1}$) using the Gibbs−Helmholtz equation (eq S3 in the Supporting Information). For DMS, a K_1^{333} of 13.4 ± 0.4 M^{-1} was found at 333 K from linear regression with $\Delta H_{f,1} = -15.0 \pm 0.7$ kJ mol^{-1} and $\Delta S_{f,1} = -23.3 \pm 2$ J mol^{-1} K^{-1}. The complex with CH_3CN exhibits a somewhat weaker stability, as indicated by its K_1^{333} of 2.5 ± 0.2 M^{-1} with the corresponding $\Delta H_{f,1} = -13.8 \pm 1$ kJ mol^{-1} and $\Delta S_{f,1} = -33.8 \pm 5$ J mol^{-1} K^{-1}.
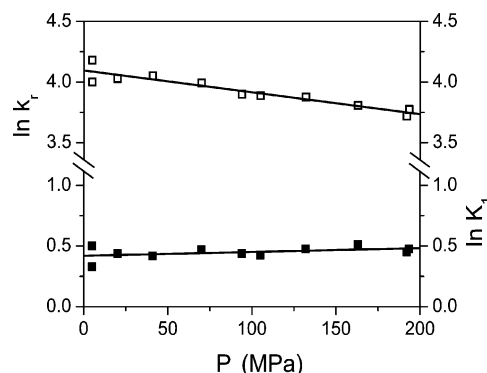
Figure 3. Complex dissociation (k_r, □) and equilibrium constant (K_1, ■) as a function of pressure for the reaction between $[(CO)_3Mn(H_2O)_3]^+$ and CH_3CN at 339.8 K and $[H^+] = 0.1$ M.

Variable-pressure experiments were performed at 339.8 K to determine the volume profiles for ligand substitution with CH_3CN and DMS by ^1H NMR (Tables S11 and S12 in the Supporting Information). In the case of CH_3CN, the population of the coordinated ligand is much smaller than that of the free ligand. The line broadening of the coordinated ligand was therefore larger and allowed a direct determination of the volume of activation for complex dissociation ($\Delta V_r^{\ddagger} = +5.1 \pm 0.6$ cm^3 mol^{-1}) using eq 6 (Figure 3). For the free ligand, the line broadening was to small to be useful. However, the pressure dependence of the equilibrium constant (eq 13 and Figure 3) could be determined from the free and coordinated CH_3CN integrals, leading to the reaction volume ($\Delta V^{\circ} = -0.9 \pm 0.6$ cm^3 mol^{-1}) and finally to the whole reaction profile (by difference: $\Delta V_f^{\ddagger} = +4.2 \pm 1.2$ cm^3 mol^{-1}).

$$(K_1)_P = (K_1)_0 \exp\left(-\frac{P\Delta V^{\circ}}{RT}\right) \qquad (13)$$

In the case of DMS, the line broadenings of the signals of free and coordinated ligands were both sufficient to determine reliably the exchange rates from them. However, reliable integration of the signal of bound DMS was difficult, resulting in a marked dispersion of the K_1^P values with the consequence of a less accurately defined reaction volume. To circumvent this problem, a simultaneous fit of k_f^P, k_r^P, and K_1^P was performed with the largest weight on k_f^P values because they have the best quality. This procedure yielded the following values: $\Delta V_f^{\ddagger} = +11.3 \pm 0.6$ cm^3 mol^{-1}, $\Delta V_r^{\ddagger} = +13.5 \pm 1.3$ cm^3 mol^{-1}, and $\Delta V^{\circ} = -2.2 \pm 1.3$ cm^3 mol^{-1}.

Water Exchange Kinetics on $[(CO)_3Tc(H_2O)_3]^+$. The half-life for the water exchange on $[(CO)_3Tc(H_2O)_3]^+$ had been estimated to lie between 1 s and 1 min at 277 K.[6] This is clearly too slow to show a detectable line broadening at this temperature. As a consequence, the water exchange rate was studied using a fast-injection device[15] at 277 K. ^{17}O-enriched water was injected in a solution of the complex and Mn^{2+} (0.2 M), and then the enrichment of the coordinated water was followed by ^{17}O NMR (Figure S3 in the Supporting Information). The experiment was repeated at three different acid concentrations and at constant ionic strength (1 M, $NaClO_4$). The observed water exchange rate
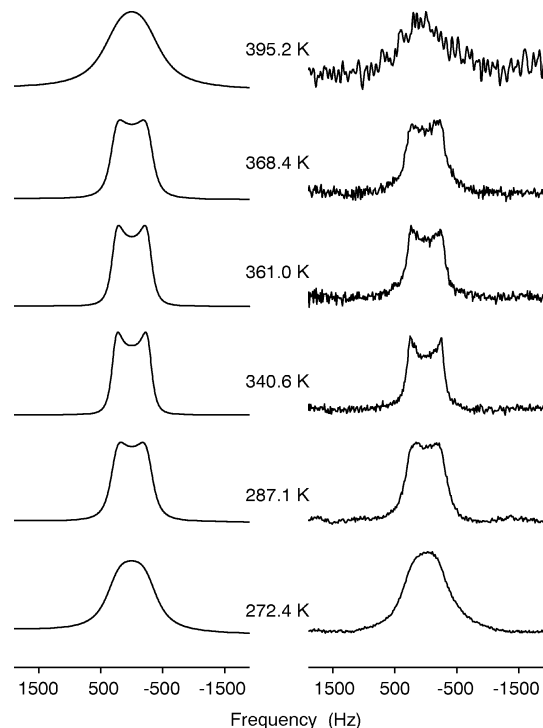
Figure 4. Calculated (left) and experimental (right) ¹⁷O NMR spectra (54 MHz) showing the signal of bound water in [(CO)₃Tc(H₂O)₃]⁺ as a function of temperature. Mn(II) was added to remove the signal of bulk water.

constants k_{obs} were 41 ± 2 s⁻¹ (p[H⁺] = 1.4), 43 ± 2 s⁻¹ (p[H⁺] = 4.3), and 42 ± 2 s⁻¹ (p[H⁺] = 4.3, PIPBS buffer) (Figure S4 in the Supporting Information). No evidence for a p[H⁺]-dependent water exchange rate in the domain covered (1.4 < p[H⁺] < 4.4) was thus observed, and a mean value of $k_{ex}^{277} = (42 \pm 2) \times 10^3$ s⁻¹ is reported. To allow a comparison with the data available for the Mn and Re homologues, the water exchange rate at 298 K is of interest, but it is directly accessible neither by the fast-injection technique nor by line broadening at this temperature. At higher temperature, kinetic effects are observable on the line shape of the bound water signal. For this purpose, ¹⁷O NMR spectra of a [(CO)₃Tc(H₂O)₃]⁺ solution in 0.1 M HClO₄ were recorded in the temperature range 272−396 K. Compared to the Mn homologue presented previously (vide supra), the evolution of the line width with the temperature is more complex in the case of [(CO)₃Tc(H₂O)₃]⁺. The line shape of the ¹⁷O NMR signal changed from a large bump to a rounded rectangular shape, whose corners became sharper and grew higher to form an "M"-shaped signal, which transformed then again to a bump at the highest temperature (Figure 4). This unusual behavior is the result of the coupling between the observed ¹⁷O nucleus and the ⁹⁹Tc nucleus ($I = \frac{9}{2}$) to which it is bound directly. Typically, the NMR signal of a nucleus that is spin−spin-coupled to another nucleus of a spin I is expected to have a multiplet structure of $2I + 1$ equally spaced lines. However, when the spin I is greater than $\frac{1}{2}$, its electric quadrupole moment will influence the shape of the multiplet due to quadrupolar relaxation. The latter being usually fast, the multiplet is generally collapsed to a single line. When the quadrupole moment is small or the nucleus with spin $I > \frac{1}{2}$ is in a highly symmetric

environment, the multiplet, or at least only a partially collapsed one, can be observed. This observation can be described using the following formalism.

The transition probabilities between the $m = 2I + 1$ ($I > \frac{1}{2}$) states due to quadrupole relaxation have been derived by Pople[22] and are given explicitly by Gillespie and co-workers.[23] Equations 14 and 15 give respectively the probabilities for one-quantum and two-quantum transitions,

$$P_{m,m\pm1} = \frac{3}{20} \frac{(2m \pm 1)^2(I \pm m + 1)(I \mp m)}{4I^2(2I-1)^2}\left(\frac{e^2qQ}{\hbar}\right)^2\tau_q \quad (14)$$

$$P_{m,m\pm2} = \frac{3}{20} \frac{(I \mp m)(I \mp m - 1)(I \pm m + 1)(I \pm m + 2)}{4I^2(2I-1)^2}\left(\frac{e^2qQ}{\hbar}\right)^2\tau_q \quad (15)$$

where eq, eQ, and τ_q are respectively the electric field gradient at the nucleus, the quadrupole moment at the nucleus, and the correlation time for molecular reorientation. The last one is proportional to the nuclear spin−lattice relaxation rate, $1/T_{1Q}$, for quadrupolar nuclei in the extreme narrowing range (eq 16).

$$\frac{1}{T_{1Q}} = \frac{3}{40} \frac{2I+3}{I^2(2I-1)}\left(\frac{e^2qQ}{\hbar}\right)^2\tau_q \quad (16)$$

The line shape of the multiplet is given by eq 17,[24]

$$\text{Int}(\omega) \propto \text{re}\{\mathbf{W}\mathbf{A}^{-1}\mathbf{1}\} \quad (17)$$

where $\mathbf{W}$ is a column vector with the population of the states and $\mathbf{1}$ a unity line vector. $\mathbf{A}$ is the complex matrix whose elements are defined by eqs 18 and 19,

$$A_{m,m} = i[(\omega_0 - \omega) + m2\pi J] - \frac{1}{\tau_m} - \frac{1}{T_{2obs}} \quad (18)$$

where $1/\tau_m$ is the inverse lifetime of each state m and is given

$$A_{m,n} = P_{m,n} \qquad m \neq n \quad (19)$$

by eq 20 and $1/T_{2obs}$ is defined in eq 2.

$$\frac{1}{\tau_m} = \sum_{\substack{n \\ n \neq m}} P_{m,n} \quad (20)$$

The nonzero elements of the 10×10 matrix for $I = \frac{9}{2}$ are given explicitly in the Supporting Information. Using this matrix and the module for the fitting of exchange processes with the Kubo−Sack[25] formalism of NMRICMA,[18] it was possible to extract from the spectra recorded at different temperatures $1/T_{1Q}$ for ⁹⁹Tc and $1/T_2$ for ¹⁷O (Table S13 in the Supporting Information). The coupling constant $J_{^{17}O-^{99}Tc}$ was determined by a manual trial-and-error procedure and

(22) Pople, J. A. *Mol. Phys.* **1958**, *1*, 168.
(23) Bacon, J.; Gillespie, R. J.; Quail, J. W. *Can. J. Chem.* **1963**, *41*, 3063.
(24) Abragam, A. *The Principle of Nuclear Magnetism*; Oxford University Press: Oxford, U.K., 1961.
(25) Johnson, C. S.; Moreland, C. G. *J. Chem. Educ.* **1973**, *50*, 477.
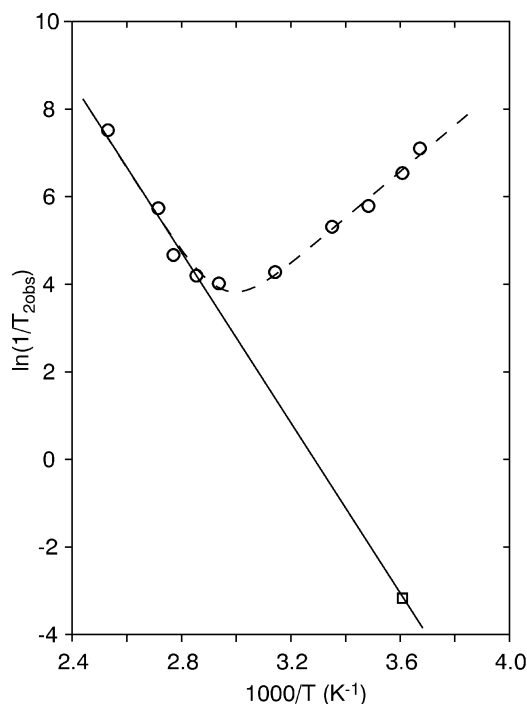
Figure 5. Transverse relaxation rate ($1/T_{2obs}$) temperature dependence of the ^{17}O NMR signal of bound water in $[(CO)_3Tc(H_2O)_3]^+$. The dashed line represents the best fit of eq 2 to $\ln(1/T_{2obs})$ experimental points (○). The solid line corresponds to the Eyring equation (eq S1 in the Supporting Information) including the $\ln(k_{ex}^{277})$ value (□).

was found to be 80 ± 5 Hz. The temperature dependence of $1/T_2$ for ^{17}O shows the usual V shape (Figure 5) corresponding to a line width controlled by quadrupolar relaxation at low temperature and by a chemical exchange process at higher temperatures (eq 2 and eqs S1 and S2 in the Supporting Information). The evolution of $1/T_1$ for ^{99}Tc with temperature is less straightforward. The ^{99}Tc NMR spectra recorded in parallel with the ^{17}O NMR spectra show that $1/T_{1Q}$ for ^{99}Tc is not directly accessible from $1/T_2$ in ^{99}Tc NMR because the line shape is also influenced by coupling to ^{17}O and chemical exchange (Figure 6). In a 10% ^{17}O-enriched solution, about 30% of the Tc nuclei are bound to ^{17}O nuclei, yielding the following isotopomer $[(CO)_3Tc(H_2^{17}O)(H_2^{16}O)_2]^+$. This isotopomer therefore appears as a broad collapsed sextet in a manner similar to that previously observed in ^{17}O NMR. Superimposed on this broad signal, a tall singlet corresponding to $[(CO)_3Tc(H_2^{16}O)_3]^+$ is observed. The Tc nucleus moves between two environments, $[(CO)_3Tc(H_2^{17}O)(H_2^{16}O)_2]^+$ and $[(CO)_3Tc(H_2^{16}O)_3]^+$, as chemical exchange proceeds, thus broadening the tall singlet.

Despite all of these complications, ^{17}O NMR spectroscopy allowed us to determine the activation parameters for the water exchange accurately as a result of the wide temperature range covered (Table S3 in the Supporting Information). For the measurements above the boiling point of water, a sapphire NMR tube[26] was used. The water exchange rate at 277 K, determined independently by the fast-injection experiment, was introduced in the fitting procedure as a fixed parameter. The following values were obtained: $k_{ex}^{298} = 0.49 \pm 0.05$
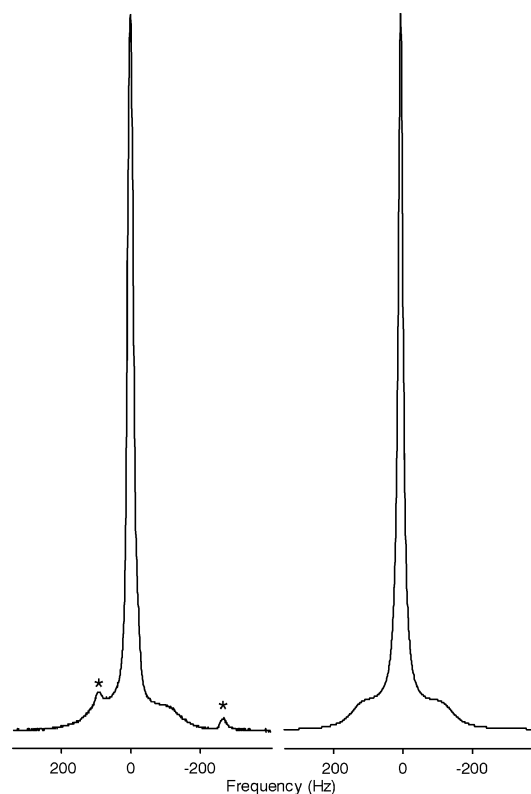
Figure 6. Experimental (left) and calculated (right) ^{99}Tc NMR spectra (90 MHz) of a solution containing $[(CO)_3Tc(H_2O)_3]^+$ in 10% ^{17}O-enriched water at 321 K: (*) ^{13}C satellites. Calculated spectrum assuming coupling to the ^{17}O nucleus ($I = {}^5/_2$). The tall signal corresponds to $[(CO)_3Tc(H_2^{16}O)_3]^+$; the signal of $[(CO)_3Tc(H_2^{17}O)(H_2^{16}O)_2]^+$ appears as a single broad signal due to partial decoupling from the ^{17}O nucleus, resulting from the quadrupolar relaxation of the latter.

s^{-1}, $\Delta H_{ex}^{\ddagger} = 78.3 \pm 1$ kJ mol^{-1}, $\Delta S_{ex}^{\ddagger} = +11.7 \pm 3$ J K^{-1} mol^{-1}, $E_Q = 43.9 \pm 4$ kJ mol^{-1}, and $1/T_{2Q} = 196 \pm 20$ s^{-1}.

Above 360 K, the complex started to decompose slowly (oxidation by ClO_4^-), and a peak at 0 ppm in ^{99}Tc NMR escorted by a small sextet ($J_{Tc-O} = 131.4$ Hz) and a peak at 747 ppm in ^{17}O NMR escorted by a decet ($J_{O-Tc} = 132.9$ Hz) were observed and assigned to TcO_4^- in accordance with data reported elsewhere.[27]

At temperatures below 380 K, the ^{17}O NMR spectrum of coordinated water is not very sensitive to the variation of the water exchange rate constant, k_{ex} (Figure 4). With the effect of the pressure on k_{ex} being much smaller than the effect of the temperature, it is necessary to work at even higher temperatures for the determination of the activation volume, $\Delta V^{\ddagger}$. To minimize the problem of decomposition of the complex, the ClO_4^- counterion was replaced by the $CF_3SO_3^-$ ion. A 0.15 M $[(CO)_3Tc(H_2O)_3]^+$ and 0.10 M CF_3SO_3H 30% ^{17}O-enriched aqueous solution gave reasonable S/N spectra at 404.6 K. Each spectrum is the result of ~16 000 scans: three spectra were taken by increasing the pressure and three by decreasing the pressure to check reversibility, and the free water signal was suppressed by the 1, −3, 3, −1 pulse sequence.[13] Exchange rate constants were obtained by fitting the spectra as described above for

(26) Cusanelli, T.; Frey, U.; Richens, D. T.; Merbach, A. E. *J. Am. Chem. Soc.* **1996**, *118*, 5265.

(27) Cho, H.; de Jong, W. A.; McNamara, B. K.; Rapko, B. M.; Burgeson, I. E. *J. Am. Chem. Soc.* **2004**, *126*, 11583.
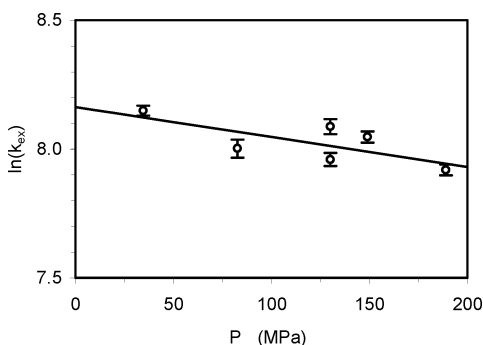
Figure 7. Pressure dependence of the water exchange rate constant, k_{ex}, on $[(CO)_3Tc(H_2O)_3]^+$ measured by ^{17}O NMR at 404.6 K.

the temperature dependence. The slight decrease observed for k_{ex} results in a positive $\Delta V^\ddagger$ of $+3.8 \pm 2$ cm^3 mol^{-1} (Figures 7 and S5 and Table S14 in the Supporting Information) and is indicative of a dissociative interchange I_d mechanism.

^{99}Tc NMR of $[(CO)_3TcL_x(H_2O)_{3-x}]^+$ Complexes (L = DMS, CH₃CN; $x = 0-3$). Although ^{99}Tc is a quadrupolar nucleus ($I = ^9/_2$), ^{99}Tc NMR is a convenient method to investigate Tc complexes because chemical shifts are strongly dependent not only on the oxidation state but also on the ligands within a particular oxidation state.[28] Signal line widths in symmetric complexes, especially in T_d or O_h symmetry, are small with a few hertz (3 Hz for TcO₄⁻).[29] The signal of Tc₂(CO)₁₀ appears at -2477 ppm (TcO₄⁻ at 0 ppm for referencing chemical shifts in ^{99}Tc NMR), and $[(CO)_3Tc(H_2O)_3]^+$ is found at -868 ppm, a relatively high value for technetium carbonyl complexes likely to be a result of strong π back-donation to the carbonyl ligands. A weak interaction of the water with Tc center is reflected by a relatively small coupling constant of 80 Hz and by the smaller isotope shift (-0.20 ppm) due to ^{18}O substitution (see Figures S6 and S7 in the Supporting Information) compared to TcO₄⁻ (132.1 Hz with respect to -0.427 ppm).[27] Thus, introducing a better donor than water in the first coordination sphere should increase the electron density at the metal and shift the ^{99}Tc NMR signal to higher fields. Like the Mn and Re homologues, water ligands on $[(CO)_3Tc-(H_2O)_3]^+$ can be easily substituted by the DMS (see Figure S8 in the Supporting Information) and CH₃CN ligands. Upon substitution of water by one of these ligands, the ^{99}Tc NMR chemical shifts drop to -907 and -911 ppm, respectively. A significant difference between the two ligands is only observed when two (DMS, -1023 ppm; CH₃CN, -981 ppm) or three (DMS, -1230 ppm; CH₃CN, -1098 ppm) water molecules are substituted. The DMS induces a stronger shielding than the CH₃CN ligand, thus showing its greater donor ability. The shift observed for $[(CO)_3Tc(DMS)_3]^+$ (-1230 ppm) remains inferior to those reported for complexes with tridentate cyclic thioethers $[(CO)_3Tc(9\text{-ane-}S_3)]^+$, -1656 ppm, and $[\{(CO)_3Tc\}_2(20\text{-ane-}S_6\text{-OH})]^+$, -1474

ppm.[30] The increased shielding of the cyclic ligands may be related to a chelate effect on the electron density. The increased shielding in the presence of chelating phosphines in comparison with monodentate phosphines has also been reported earlier.[31]

The mono- and bisubstituted complexes have line widths of several hundred hertz compared to a few tens of hertz of the tris complexes (Table S15 in the Supporting Information). This is a smart illustration of how the higher symmetry of the "tris complexes" compared to the "bis complexes" affects the quadrupolar relaxation of the ^{99}Tc nucleus.

Water Substitution Kinetics on $[(CO)_3Tc(H_2O)_3]^+$. The fast-injection technique was used to study the substitution of water by the ligands CH₃CN and DMS (Figure S9 in the Supporting Information). For each ligand, the reaction was monitored at three temperatures by ^{99}Tc NMR. This was more suitable than ^1H NMR because of the faster relaxation of the quadrupolar ^{99}Tc nucleus. Once equilibrium was reached, ^1H NMR spectra were recorded to determine the concentration of the free ligand for calculation of the equilibrium constants. The complex with DMS exhibits a higher stability than that with CH₃CN ($K_1^{277} = 18.3 \pm 0.1$ M^{-1} vs $K_1^{277} = 3.0 \pm 0.1$ M^{-1}). The corresponding reaction enthalpies and entropies are $\Delta H_{f,1} = -6.8 \pm 0.3$ kJ mol^{-1} and $\Delta S_{f,1} = -0.3 \pm 0.9$ J mol^{-1} K^{-1} for DMS and $\Delta H_{f,1} = -0.7 \pm 0.8$ kJ mol^{-1} and $\Delta S_{f,1} = +6.5 \pm 3$ J mol^{-1} K^{-1} for CH₃CN (Figure S10 and Tables S16 and S17 in the Supporting Information).

The complex formation rate constants with DMS are twice as high as those with CH₃CN, respectively $k_{f,1}^{277} = (6.67 \pm 0.03) \times 10^{-3}$ and $(3.43 \pm 0.01) \times 10^{-3}$ mol^{-1} s^{-1}. The corresponding enthalpies and entropies are $\Delta H_{f,1}^\ddagger = 70.6 \pm 3$ kJ mol^{-1}, $\Delta S_{f,1}^\ddagger = -31.1 \pm 10$ J mol^{-1} K^{-1} and $\Delta H_{f,1}^\ddagger = 77.8 \pm 8$ kJ mol^{-1}, $\Delta S_{f,1}^\ddagger = -10 \pm 27$ J mol^{-1} K^{-1}, respectively.

Water Substitution Kinetics on $[(CO)_3Re(H_2O)_3]^+$. The reactivity of $[(CO)_3Re(H_2O)_3]^+$ toward several ligands had already been studied at 298 K.[4,5] Here, to extend this study, the water substitution by CH₃CN at two other temperatures has been investigated to determine the thermodynamic and activation parameters to allow comparison with the Mn and Tc analogues. For Re, the activation parameters are $\Delta H_{f,1}^\ddagger = 98.6 \pm 3$ kJ mol^{-1} and $\Delta S_{f,1}^\ddagger = +26.6 \pm 10$ J mol^{-1} K^{-1}. The corresponding reaction enthalpy and entropy are $\Delta H_{f,1} = -12.3 \pm 1$ kJ mol^{-1} and $\Delta S_{f,1} = -28.4 \pm 4$ J mol^{-1} K^{-1} (Table S18 in the Supporting Information).

Discussion

Spectroscopic Characteristics of Aquacarbonyl Complexes of Mn, Tc, and Re. IR carbonyl stretching frequencies and ^{13}C and ^{17}O NMR chemical shifts (δ_C and δ_O) show trends within group 7. These trends are also observed in the neighboring groups 6 and 8, although the data sets are less complete (Table 1). The IR frequencies increase clearly with

(28) Alberto, R. Technetium. In *Comprehensive Coordination Chemistry II*; McCleverty, J. A., Meyer, T. J., Eds.; Elsevier Pergamon: Amsterdam, The Netherlands, 2004; Vol. 5.

(29) Buckingham, M. J.; Hawkes, G. E.; Thornback, J. R. *Inorg. Chim. Acta* **1981**, *56*, L41.

(30) Schibli, R.; Alberto, R.; Abram, U.; Abram, S.; Egli, A.; Schubiger, P. A.; Kaden, T. A. *Inorg. Chem.* **1998**, *37*, 3509.

(31) Findeisen, M.; Kaden, L.; Lorenz, B.; Wahren, M. *Inorg. Chim. Acta* **1988**, *142*, 3.

Table 1. Comparison of Carbonyl IR and ^{13}C NMR Data for Triaquacarbonyl (ν_{CO}: A_1/E) [6,10,11,36] and Hexacarbonyl[32] (in Brackets) Complexes of Groups 6−8 Metals

	group 6		group 7		group 8	
	Cr(0)		Mn(I)		Fe(II)	
ν_{CO} (cm^{-1})	1778/1912	(2000)	1944/2051	(2100)		(2203)
δ_C (ppm)		(212)	223	(195)		(179)
	Mo(0)		Tc(I)		Ru(II)	
ν_{CO} (cm^{-1})		(2004)	1936/2051	(2051)	2089/2156	(2198)
δ_C (ppm)		(204)	210	(190)	182	(166)
	W(0)		Re(I)		Os(II)	
ν_{CO} (cm^{-1})	1916/2012	(1998)	1916/2037	(2084)		(2190)
δ_C (ppm)		(192)	183	(171)		(147)
ν_{CO}						
δ_C, π back-bonding						

Figure 8. NMR shifts for [(CO)$_3$M(H$_2$O)$_3$]$^+$, in order of decreasing frequency: ^{17}O carbonyl, ^{13}C carbonyl, and ^{17}O water.

charge and show a small trend to decrease within a group from top to bottom for these isoelectronic tricarbonyltriaqua complexes (t_{2g}^6). The same behavior has been reported for the homoleptic hexacarbonyl complexes of groups 6−8 and reflects well the variable extent of π back-bonding in the different complexes.[32] The highly positively charged complexes, where carbonyl acts mainly as a σ donor, display higher frequencies than electron-rich neutral complexes, where carbonyl acts as a strong π acid. The aquacarbonyl complexes can be seen as hexacarbonyls, with three carbonyl ligands being replaced by purely σ-donating water molecules. These three remaining carbonyl ligands experience stronger π back-bonding and correspondingly lower carbonyl stretching frequencies. The efficient π back-bonding is certainly the reason these low-valent aqua ions are stable toward oxidation. The existence of the corresponding t_{2g}^6 hexaaqua ions seems rather improbable except for Ru(II), which has been known for several years now but is very sensitive to oxidation.[33]

The chemical shift δ_C is also controlled by the balance between σ donation and π back-bonding. It decreases with increasing atomic number as well in a row as along the period. The effect of σ donation and π back-bonding on the shielding of the ^{13}C nucleus has been studied by density functional theory (DFT).[34] These calculations showed that in the case of the hexacarbonyl complexes the π back-bonding has a positive contribution whereas σ donation has a negative contribution to the chemical shift. These contributions originate mainly from the paramagnetic coupling between occupied and virtual orbitals. With the manganese, technetium, rhenium, and ruthenium aquacarbonyl complexes having higher δ_C than the analogous hexacarbonyl complexes, the π back-bonding is stronger and thus confirms the conclusion drawn from the IR data. The decrease of δ_C within a group is explained by the stabilization of the s and p orbitals, especially in the case of the third row, where relativistic effects are involved, which make them more
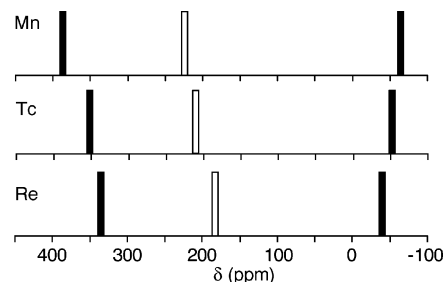
accessible for σ donation, with the latter contributing negatively to the chemical shift.[34] In group 7, δ_O of the carbonyl ligands follow the same trend as δ_C (Figure 8). Thus, it appears that the negative contribution of σ donation to the chemical shift applies also to the ^{17}O nucleus. Actually, DFT calculations have shown that in metal hexacarbonyl complexes the shieldings of ^{13}C and ^{17}O follow the same trends.[35] The increase of δ_O when going from Tc (352 ppm) to Ru (370 ppm)[36] does not fit the trend observed for δ_C. Unfortunately, to our knowledge, no data are available for other aquacarbonyl complexes to extend the comparison.

An intuitive way to account for the variation of the ^{17}O chemical shifts of bound water is to consider that an enhanced metal carbonyl π back-bonding increases the electrophilicity of the metal. Thus, the σ donation of the water ligand is increased, which depletes the electron density at the O atom of the water ligand, inducing therefore a deshielding of the ^{17}O nucleus of bound water. In conclusion, when going down group 7, the metal acts increasingly as an electron pump, transferring electron density from the water ligands, through the metal, onto the carbonyl ligands therefore increasing the metal−water bond strength.

Oxygen Exchange on the Carbonyl Ligand. Since the report by Muetterties, showing that [Re(CO)$_6$]$^+$ exchanges its O atom with water without being decomposed,[37] this reaction has been qualitatively studied by IR.[38] Later, a ^{17}O NMR study provided quantitative data.[39] The oxygen exchange on [Re(CO)$_6$]PF$_6$ in H$_2$O/CH$_3$CN was assumed to obey the following rate law: rate = k_{CO}[Re(CO)$_6^+$][H$_2$O]^2 with k_{CO}^{305} = (5.84 ± 0.90) × 10^{-4} M^{-2} s^{-1}. A similar oxygen exchange has also been reported for [(CO)$_x$Ru(H$_2$O)$_{6-x}$]$^{2+}$ complexes ($x = 1-3$), where the rates increase with increasing x.[36] For $x = 1$, only an upper limit for k_{CO} was reported, $k_{CO}^{353} \leq 1 \times 10^{-8}$ s^{-1}, and no acidity dependence was observed. In the bicarbonyl complex ($x = 2$), a slight acidity dependence was observed but was not further investigated. The reported value is k_{CO}^{313} = (1.18 ± 0.03) × 10^{-4} s^{-1}. In the case of the comparatively very acidic (pK_a −0.14) tricarbonyl complex ($x = 3$), a clear increase

(32) Willner, H.; Aubke, F. *Angew. Chem., Int. Ed.* **1997**, *36*, 2402.
(33) Bernhard, P.; Bürgi, H.-B.; Hauser, J.; Lehmann, H.; Ludi, A. *Inorg. Chem.* **1982**, *21*, 3936.
(34) Ehlers, A. W.; Ruiz-Morales, Y.; Baerends, E. J.; Ziegler, T. *Inorg. Chem.* **1997**, *36*, 5031.
(35) Ruiz-Morales, Y.; Schreckenbach, G.; Ziegler, T. *J. Phys. Chem.* **1996**, *36*, 3359.
(36) (a) Meier, U. C.; Scopelliti, R.; Solari, E.; Merbach, A. E. *Inorg. Chem.* **2000**, *39*, 3816. (b) Alberto, R.; Schibli, R.; Egli, A.; Schubiger, P. A.; Herrmann, W. A.; Abram, U.; Kaden, Th. A. *J. Organomet. Chem.* **1995**, *493*, 119.
(37) Muetterties, E. L. *Inorg. Chem.* **1965**, *4*, 1841.
(38) Darensbourg, D. J.; Froelich, J. A. *J. Am. Chem. Soc.* **1977**, *99*, 4726.
(39) Kump, R. L.; Todd, L. J. *Inorg. Chem.* **1981**, *20*, 3715.

Table 2. Selected Kinetic Data and Mechanisms of Water Exchange for Aqua Complexes of Cr(0), W(0), Mn(I), Tc(I), Re(I), Ru(II), Os(II), Co(III), Rh(III), and Ir(III) at 298 K, Including Acid Dissociation Constants and Water ^{17}O NMR Chemical Shifts

	k_{ex}^{298} (s^{-1})	$\Delta H_{ex}^{\ddagger}$ (kJ mol^{-1})	$\Delta S_{ex}^{\ddagger}$ (J mol^{-1} K^{-1})	$\Delta V_{ex}^{\ddagger}$ (cm^3 mol^{-1})	mechanism	pK_a	δ ^{17}O	ref
[(CO)$_3$Cr(H$_2$O)$_3$]	11×10^4	50	+20			<8	15	11
[(CO)$_3$W(H$_2$O)$_3$]	31	58	−22			<4.5	−8	11
[(CO)$_3$Mn(H$_2$O)$_3$]$^+$	23	72.5	+24.4	+7.1	I$_d$	9−10	−65	this work
[(CO)$_3$Tc(H$_2$O)$_3$]$^+$	0.49	78.3	+11.7	+3.8	I$_d$		−52	this work
[(CO)$_3$Re(H$_2$O)$_3$]$^+$	5.4×10^{-3}	90.3	+14.5		I$_d$	7.5	−40	5
[(CO)$_3$Re(OH)(H$_2$O)$_2$]	27							5
[Ru(H$_2$O)$_6$]$^{2+}$	1.8×10^{-2}	87.8	+16.1	−0.4	I$_d$	6−8	−196.3	46
[(CO)$_3$Ru(H$_2$O)$_3$]$^{2+}$	10^{-4}–10^{-3}					−0.14	−68	36
[(CO)$_3$Ru(OH)(H$_2$O)$_3$]$^+$	$5.3 \times 10^{-2\,a}$							36
[(η^6-C$_6$H$_6$)Ru(H$_2$O)$_3$]$^{2+}$	11.5	75.9	+29.9	+1.5	I$_d$	3.5	−73.4	42
[(η^6-C$_6$H$_6$)Os(H$_2$O)$_3$]$^{2+}$	11.8	65.5	−4.8	+2.9	I$_d$		−66.6	42
[Co(H$_2$O)$_6$]$^{3+}$	$\leq 1 \times 10^3$					1.7		43
[Cp*Co(H$_2$O)$_3$]$^{2+}$	60							44
[Rh(H$_2$O)$_6$]$^{3+}$	2.2×10^{-9}	131	+29	−4.2	I$_a$	3.5	−130.5	47
[Rh(OH)(H$_2$O)$_5$]$^{2+}$	4.2×10^{-5}	103		+1.5	I			47
[Cp*Rh(H$_2$O)$_3$]$^{2+}$	1.6×10^5	65.6	+75.3	+0.6	I$_d$	5.3^b	−64	44
[Ir(H$_2$O)$_6$]$^{3+}$	1.1×10^{-10}	130.5	+2.1	−5.7	I$_a$	4.45	−151	26
[Ir(OH)(H$_2$O)$_5$]$^{2+}$	5.6×10^{-7}			+1.3	I			26
[Cp*Ir(H$_2$O)$_3$]$^{2+}$	2.53×10^4	54.9	+23.6	+2.4	I$_d$		−60	44

^{a} At 262 K. ^{b} Deprotonation is instantly followed by dimerization.[45]

of the exchange rate with decreasing acidity was observed. Exchange rates on protonated [$k_{CO}^{262} = (3 \pm 2) \times 10^{-3}$ s^{-1}] and deprotonated [$k_{CO}^{262,OH} = (24 \pm 3) \times 10^{-3}$ s^{-1}] aqua complexes were determined.[36]

Now, quantitative data for the oxygen exchange on the carbonyl ligand of [(CO)$_3$Mn(H$_2$O)$_3$]$^+$ have been obtained. The reaction, with $k_{CO}^{338} = (4.3 \pm 0.2) \times 10^{-6}$ s^{-1}, is slower than that for the Ru(II) analogue complex. For the Tc homologue, a slight enrichment has been observed after heating the solution above 390 K for more than 2 h, but for the Re homologue, no exchange at all has been observed, even when the complex was kept for several days in an ^{17}O-enriched acidic aqueous solution and heated. Thus, the ability of group 7 triaquacarbonyl complexes to exchange the O atoms of carbonyl decreases down the group, in parallel with the increase of π back-bonding as reflected by the carbonyl stretching frequencies. This is not surprising if one looks at the mechanism of oxygen exchange.

Generally, it is assumed that the oxygen exchange on carbonyl ligands in the presence of water proceeds via a so-called metallacarboxylic acid, which is the result of nucleophilic attack of H$_2$O (or OH$^-$) on the C atom of the carbonyl ligand.[36−40] An electron-depleted carbonyl will therefore be more prone for nucleophilic attack than a carbonyl experiencing a strong π back-bonding. Among the complexes discussed here, [(CO)$_3$Ru(H$_2$O)$_3$]$^{2+}$ has one of the highest frequencies and is also the complex with the fastest exchange.[36] However, [Re(CO)$_6$]$^+$ with almost the same frequency is less reactive, likely owing to its lower charge. Finally, [(CO)$_3$Mn(H$_2$O)$_3$]$^+$, being at the lower end of the range, belongs also to the slowest exchanging complexes.

From these observations, it is possible to predict that [Mn(CO)$_6$]$^+$ and [Tc(CO)$_6$]$^+$ should also undergo observable oxygen exchange on their carbonyl ligands. Actually, ^{17}O NMR signals that can be assigned to enriched carbonyl ligands have been observed in a solution of [(CO)$_3$Tc(H$_2$O)$_3$]$^+$ that was pressurized with carbonyl and where [Tc(CO)$_6$]$^+$, as well as [(CO)$_4$Tc(H$_2$O)$_2$]$^+$ and [(CO)$_5$Tc(H$_2$O)]$^+$, have been observed.[6]

The decomposition of [(CO)$_3$Mn(H$_2$O)$_3$]$^+$ can be related to the reactivity of its carbonyl ligands. For [(CO)$_3$Ru(H$_2$O)$_3$]$^{2+}$, the formation of a hydride [(CO)$_2$RuH(H$_2$O)$_3$]$^+$, as a consequence of decarboxylation of the ruthenacarboxylic acid, has been reported.[41] In the Mn(I) case, no evidence was found by ^{1}H NMR for the presence of a hydride complex. However, it may be present at low concentration and thus escape detection by NMR. The presence of this hypothetical manganese hydride may explain the decomposition of [(CO)$_3$Mn(H$_2$O)$_3$]$^+$. The hydride resulting from decarboxylation would then be protonated to form a labile dihydrogen complex. Loss of H$_2$ yields an unstable "bicarbonylmanganese(II)", losing its carbonyl to form [Mn(H$_2$O)$_6$]$^{2+}$, whose presence is easily detected by NMR thanks to its paramagnetism.

Water Exchange and Complex Formation Reactions of [(CO)$_3$M(H$_2$O)$_3$]$^+$ Complexes (M = Mn, Tc, Re)

Water Exchange Rate. The water exchange rates decrease when going down within group 7 (Table 2). The rates also decrease in a row from one group to the next. Thus, within a period, the decrease of the water exchange rate is paralleled by a charge increase of these isoelectronic (t$_{2g}^6$) complexes. Such a lability decrease has already been reported for the isoelectronic [Ru(H$_2$O)$_6$]$^{2+}$ and [Rh(H$_2$O)$_6$]$^{3+}$ aqua ions,[46,47] where the increased bond strength leads even to a change in the water exchange mechanism from I$_d$ to I$_a$.[48] Thus, the electrostatic interaction is influencing the metal−water bond

(40) Bennett, M. A. *J. Mol. Catal.* **1987**, *41*, 1.
(41) Funaioli, T.; Cavazza, C.; Marchetti, F.; Fachinetti, G. *Inorg. Chem.* **1999**, *38*, 3361.
(42) Stebler-Röthlisberger, H.; Hummel, W.; Pittner, P.-A.; Bürgi, H.-B.; Ludi, A.; Merbach, A. E. *Inorg. Chem.* **1988**, *27*, 1358.
(43) Conochiolo, T. J.; Nancollas, G. H. *Inorg. Chem.* **1965**, *5*, 1.
(44) Dadci, L.; Elias, H.; Frey, U.; Hörnig, A.; Koelle, U.; Merbach, A. E.; Paulus, H.; Schneider, J. S. *Inorg. Chem.* **1995**, *34*, 306.
(45) Eisen, M. S.; Haskel, A.; Chen, H.; Olmstead, M. M.; Smith, D. P.; Maestre, M. F.; Fish, R. H. *Organometallics* **1995**, *14*, 2806.
(46) Rapaport, I.; Helm, L.; Merbach, A. E.; Bernhard, P.; Ludi, A. *Inorg. Chem.* **1988**, *27*, 873.
(47) Laurenczy, G.; Rapaport, I.; Zbinden, D.; Merbach, A. E. *Magn. Reson. Chem.* **1991**, *29*, S45.

strength, which also is clearly visible in the increased activation enthalpies for the water exchange (Table 2).

Water exchange rate variations within a group cannot be due to a modification of the formal charge. As already discussed previously (vide supra), π back-bonding is increasing when moving down the group, thus enhancing the electrophilicity of the metal, which, in turn, favors strong σ donation from the water ligand. Consequently, the water molecules are more tightly bound to the metal. This correlates with the observed decrease in lability, implying a similar transition state for water self-exchange. In the case of ruthenium(II) aquacarbonyl complexes, a decrease of the lability of the water molecules cis to the carbonyl ligand has been reported with increasing numbers of carbonyl ligands and thus with increasing π back-bonding.[36]

Only activation volumes for Mn(I) and Tc(I) are available. Their positive values are indicative of a dissociative activated water exchange process. All complexes, except the W(0) one, show positive activation entropies for this process, pointing also to an I_d mechanism.

Acidity Dependence of the Water Exchange Rate. Upon deprotonation of an aqua ion, one observes an increase of its water exchange rate by 2−4 orders of magnitude.[49] In the case of $[(CO)_3Re(H_2O)_3]^+$, the ratio k_{OH}/k_{ex} is about 5000 (Table 2). Unlike $[(CO)_3Re(H_2O)_3]^+$, no acidity-dependent variation of k_{ex} for $[(CO)_3Mn(H_2O)_3]^+$ (up to pH 6.3) and $[(CO)_3Tc(H_2O)_3]^+$ (up to pH 4.4) has been observed in the present work. Considering an envisaged pK_a of 9−10 for $[(CO)_3Mn(H_2O)_3]^+$, the ratio between the hydrolyzed species $[(CO)_3Mn(OH)(H_2O)_2]$ and $[(CO)_3Mn(H_2O)_3]^+$ is less than 1:1000 at the lowest acidity (pH 6.3) of the kinetic measurements. This allows one to calculate that the rate of water exchange on $[(CO)_3Mn(OH)(H_2O)_2]$ is not larger than 1000 times the exchange rate on the nonhydrolyzed species, which is less than that observed for Re. For Re, the ratio depends on the pK_a value, which is well-known. Unfortunately, measurements in neutral to slightly alkaline conditions to assess these conclusions could not be performed because of fast decomposition of the samples. Because the Re−O bond is stronger than the Mn−O bond, an increased acidity of the coordinated water in $[(CO)_3Re(H_2O)_3]^+$ with respect to $[(CO)_3Mn(H_2O)_3]^+$ is reasonable.

For Tc, the acidity range covered is smaller and its pK_a is still lacking. However, with $[(CO)_3Tc(H_2O)_3]^+$ having spectroscopic properties and a water exchange rate that are intermediate between those of the Mn and Re homologues, a pK_a in the range 7−9 is expected. It is therefore not surprising that no acidity dependence of the water exchange rate is observed up to pH 4.4.

Complex Formation. All three water molecules on the triaquacarbonyl complexes of Mn(I) and Tc(I) can be substituted by CH_3CN and DMS, and thus they strongly resemble the homologue Re(I) complex.[5] For the Cr(0) analogue, it has been reported that all three water

molecules can be substituted by the tridentate ligands $[CpCo(OP(OEt)_2)_3]^-$, 1,3,5-timethyl-1,3,5-triazacyclohexane, and diethylenetriamine, and thus this confirmed the facial geometry.[11] The bipyridine ligand substitutes two water molecules in the W(0) and Mn(I) complexes[11] in a similar way as it does in the Re(I) complex.[5] For Ru(II), no data about water substitution are available at present.

Both thermodynamic and kinetic data are only available for Mn, Tc, and Re; thus, the discussion will be mainly focused on the complexes of group 7 (Table 3). For all three metals, the complexes are more stable with DMS than with CH_3CN. However, the differences in stability decrease when going down the group, and this is the result of the decreasing stability of the DMS complexes.

The variable affinity of the metals for the two ligands is also visible in the evolution of the kinetic parameters down the group. The substitution by DMS is only slightly faster than that by CH_3CN. In the case of Mn, the substitution rate by DMS is 4 times larger than that by CH_3CN. The ratio is only 1.5 for Tc and 1.2 for Re.

A direct comparison between complex formation, $k_{f,1}$, and water exchange, k_{ex}, rate constants is only possible when the Eigen−Wilkins model[50] describing the substitution mechanisms on octahedral complexes is considered. This model assumes that the encounter of the metal complex and the ligand is diffusion-controlled and thermodynamically quantified by the equilibrium constant K_{os}. The following step is rate-determining and consists of the exchange of ligands between the second and first coordination spheres of the metal. The first-order rate constant, k_i, describes this last step and, thus, the overall process follows $k_f = k_i K_{os}$.

However, k_i cannot be compared to k_{ex} at this stage, and statistical factors have to be taken into account.[51] Thus, eq 21 has been proposed to compare k_i' for complex formation and k_{ex} for water exchange. f is the number of molecules in the second coordination sphere of the metal complex, whereas n_c is the number of equivalent coordinated water molecules in the first coordination sphere.

$$k_i' = \frac{k_f}{K_{os}} \frac{f}{n_c} \qquad (21)$$

Table 3 lists k_i' and k_{ex} values for Mn, Tc, and Re with DMS and CH_3CN. For all three metals, the following series is observed: $k_i'(DMS) > k_i'(CH_3CN) > k_{ex}$. For Mn and Re, a 4-fold increase between $k_i'(DMS)$ and k_{ex} is observed, whereas for Tc, it is only 2-fold. Nevertheless, these kinetic differences are small compared to what has been reported for complexes that react strictly associatively where variations of several orders of magnitude are known.[52] Consequently, the complexes under investigation here are to be set in the I_a−I_d range. Previous investigations of the Re complex provided complete reaction volume profiles. On this complex, the water substitution by the hard donor pyrazine

(48) De Vito, D.; Sidorenkova, H.; Rotzinger, F. P.; Weber, J.; Merbach, A. E. *Inorg. Chem.* **2000**, *39*, 5547.

(49) Richens, D. T. *The Chemistry of Aquaions*; John Wiley & Sons: Chichester, U.K., 1997.

(50) Eigen, M.; Tamm, K. *Z. Elektrochem.* **1962**, *66*, 93.

(51) Aebischer, N.; Churlaud, R.; Dolci, L.; Frey, U.; Merbach, A. E. *Inorg. Chem.* **1998**, *37*, 5915.

(52) Tobe, M. L.; Burgess, J. *Inorganic Reaction Mechanisms*; Longman: New York, 1999.

Table 3. Thermodynamic and Kinetic Parameters for Water Substitution on [(CO)₃M(H₂O)₃]⁺ Complexes (M = Mn, Tc, Re) at 298 K

	[(CO)₃Mn(H₂O)₃]⁺			[(CO)₃Tc(H₂O)₃]⁺			[(CO)₃Re(H₂O)₃]⁺			
	CH₃CN	DMS	H₂O	CH₃CN	DMS	H₂O	pyrazine[e]	DMS[e]	CH₃CN	H₂O[e]
K_1^{298} (M^{-1})	4.5 ± 0.2	25.2 ± 0.5		2.9 ± 0.1	14.9 ± 0.1		237 ± 15	8.3 ± 0.1	4.8 ± 0.5[e]	5.4 ± 0.2[b]
$\Delta H_{f,1}$ (kJ mol⁻¹)	−13.8 ± 1	−15.0 ± 0.7		−0.7 ± 0.8	−6.8 ± 0.3				−12.3 ± 1	
$\Delta S_{f,1}$ (J mol⁻¹ K⁻¹)	−33.8 ± 5	−23.3 ± 2		+6.5 ± 3	−0.3 ± 0.9				−28.4 ± 4	
$k_{f,1}^{298} \times 10^3$ (M^{-1} s⁻¹)	1750 ± 400[a]	5340 ± 2000[a]		39.9 ± 1	60.8 ± 0.8		1.06 ± 0.05	1.18 ± 0.06	0.76 ± 0.04[e]	
$k_i^{298} \times 10^3$ (s⁻¹)[c]	29 000[a]	89 000[a]	23 000 ± 4000[a,b]	665	1010	490 ± 50[b]	17.7	20	13	
$\Delta H_{f,1}^{\ddagger}$ (kJ mol⁻¹)	83.9 ± 5	71.2 ± 12	72.5 ± 3[d]	77.8 ± 8	70.6 ± 3	78.3 ± 1[d]	98.6 ± 3		98.6 ± 3	90.3 ± 2[d]
$\Delta S_{f,1}^{\ddagger}$ (J mol⁻¹ K⁻¹)	+41.3 ± 16	+8.1 ± 38	+24.4 ± 8[d]	−10.0 ± 27	−31.1 ± 10	+11.7 ± 3[d]			+26.6 ± 10	+14.5 ± 8[d]
$\Delta V_{f,1}^{\ddagger}$ (cm³ mol⁻¹)	+4.2 ± 1.2	+11.3 ± 0.6	+7.1 ± 2.0[d]			+3.8 ± 2[d]	+5.4 ± 1.5	−12 ± 1		

[a] Results from extrapolation outside the temperature range covered experimentally. [b] $k_{ex} \times 10^3$ (s⁻¹) rate constant for the exchange of a particular water molecule. [c] $k_i' = (k_{f,1}f)/(K_{os}n_c)$ with f = probability factor = 12, K_{os} = outer-sphere formation constant = 0.24 M⁻¹ for neutral ligands, and n_c = number of coordinated water molecules = 3. [d] Activation parameters for water exchange. [e] Reference 5.
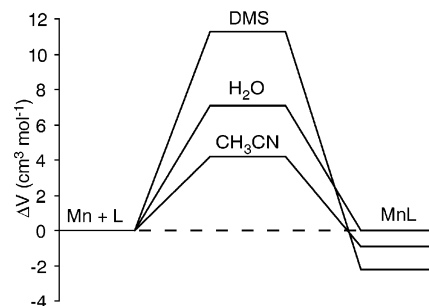
Figure 9. Volume profile for ligand substitution reactions on [(CO)₃Mn-(H₂O)₃]⁺.

is characterized by a positive activation volume, whereas for the reaction with the soft donor DMS, a negative activation volume was found.[4] From these activation volume profiles, a mechanistic changeover from I_d with the hard ligand to I_a with the soft one has been assigned for the Re complex. No activation volume for the water exchange on Re is available, but the positive activation entropy already reported[5] is compatible with an I_d mechanism, which is expected for the rather hard water ligand. The same argument holds certainly for the CH₃CN ligand, for which a positive activation entropy is reported here. In the case of [(CO)₃Mn(H₂O)₃]⁺, the pressure-dependent kinetic studies of the water exchange and complex formation with CH₃CN and soft DMS are different. As shown in the volume profiles (Figure 9), the change in volume to reach the transition state is always clearly positive, allowing one to assign for those hard and soft ligands a dissociative interchange I_d mechanism. The question now arises about the mechanistic behavior of Tc, which is between Mn (I_d) and Re (changeover I_d/I_a). The $\Delta V_{ex}^{\ddagger}$ value of +3.8 cm³ mol⁻¹ for the water exchange on [(CO)₃Tc(H₂O)₃]⁺ allows one to conclude an I_d mechanism. However, activation volumes for complex formation on this species are still necessary to provide a definitive conclusion. Its substitution behavior could follow an I_d mechanism like Mn or show an I_d/I_a mechanistic changeover driven by the hardness/softness of the incoming ligand as for Re.

Conclusions

The kinetic investigation of the water exchange and complex formation with hard and soft donors on group 7 [(CO)₃M(H₂O)₃]⁺ compounds has demonstrated that the reactivity has a small dependence on the nature of the entering ligand. However, it depends strongly on the metal center, with the following water exchange rates k_{ex} (in s⁻¹): Mn (23) > Tc (0.49) > Re (0.0054), illustrating the constant decrease of reactivity down the group. This result is of fundamental interest for a rational preparation of new *fac*-[M(CO)₃]⁺ (M = ⁹⁹ᵐTc, ¹⁸⁶/¹⁸⁸Re) based radiopharmaceuticals. After the synthesis of the immediate precursor [⁹⁹ᵐTc-(OH₂)₃(CO)₃]⁺, the three water ligands are exchanged for an incoming ligand, representing a pendant or an integrated part of a targeting biomolecule. For the preparation of new radiopharmaceuticals, these data will allow an estimation of an approximate time scale under typical conditions for a labeling process to go to completion.

Supporting Information Available: ^{17}O NMR $1/T_2$ data for water exchange on $[(CO)_3M(H_2O)_3]^+$ (M = Tc, Mn) and data analysis, ^1H NMR data for CH$_3$CN and DMS complex formation on $[(CO)_3M(H_2O)_3]^+$ (M = Tc, Mn), and ^{99}Tc NMR chemical shifts. This material is available free of charge via the Internet at http://pubs.acs.org.

IC061578Y